Optica Applicata VII/2, 1977

*A. K. Gupta, K. Singh**

Diffraction theory of image formation in presence of linear coma: incoherent annulus object

A graphical study is made of an incoherent annulus object in presence of linear (circular) coma using optical transfer function approach. Results are given in the paraxial receiving plane for various amount of coma using various sizes of the object. The loss of rotational symmetry in the resulting images is plotted and other deleterious effects of aberration discussed. Problems under investigation are outlined at the end.

1. Introduction

Considerations of off-axis aberrations of optical systems are of considerable significance in reconnaissance and survey with the help of telescopic optical instruments designed to provide maximum information on target positions in a relatively large field of view. Third order coma happens to be the most important off-axis aberration, because it varies as the first power of the object field and is first to appear when the field extends beyond the on-axis case.

Considerable work concerning the transfer function and images of various objects formed by an optical system suffering from off-axis aberrations, such as coma [1–34] and astigmatism [35–41] has already been done. MARTIN [1], STEWARD [2], NIJBOER [4], KINGSLAKE [6], and NIENHUIS and NIJBOER [7] have studied the effect of coma on the diffraction image of point objects for a circular aperture system. STEWARD [2], NIJBOER [4], and KINGSLAKE [6] have numerrically evaluated the point spread function in presence of coma, and given the results in the form of isophotes in various cases. KINGSLAKE [6] and NIENHUIS [7] present valuable photographs of the comatic images. These patterns are also reproduced in LINFOOT [11]. The main features of the comatic image for large values of coma have been discussed by VAN KAMPEN [8, 9]. KAPANY and BURKE [17] have evaluated the six image specifying parameters (i.e. point image, line image, edge image, flux through hole and slit and frequency response) used frequently for various values of the three primary aberrations (spherical, coma and astigmatism) in different focal planes. BARAKAT and HOUSTON [18,19] computed the point, line and edge images suffering from coma. ASAKURA and MISHINA [23] have treated the case of annular aperture systems in presence of coma, and obtained the results for point images. Recently ISHII and KUBOTA [30] have reported an experimental comparison of diffraction patterns of a square aperture having third order coma obtained by holographic methods with those theoretically constructed by BARAKAT and HOUSTON [18]. BISWAS and BOIVIN [32] have investigated the performance of an optical instrument equipped with an optimum apodiser in presence of primary coma. They have presented a theoretical formulation and studied the performance of apodisers in terms of the irradiance distribution and the fractional encircled energy distribution in the far-field pattern. YZUEL and BESCOS [34] have discussed the polychromatic point spread functions in presence of primary coma.

Investigations concerning the diffraction images of isolated objects are of considerable importance in reconnaissance work and photographic resolution measurements [42–45] where the objects of various shapes have been distinguished. Consequently analysis of imagery of aperiodic objects, like lines, edges, disks and annulii etc. [46–63] have gained a considerable importance. A critical analysis of different targets used in various countries for determining the photographic resolution of optical systems is given by ARTISHEVSKII and GRADOBOEV [64]. Annular targets present a considerable advantage in resolving power measurements of the system. The time of reading results is shortened, because one object caters for resolution in all directions. Annular object is, therefore, widely used as resolving power test target in aerial photography [42].

Although much attention has been paid to study the images of these extended annular targets, and the effect of partial coherence, motion, and vibration has been discussed by past workers [59, 60, 62], little work seems to have been done to study the effect of off-axis aberrations. The purpose of this paper

* The authors are with Department of Physics Indian Institute of Technology New Delhi-110029.

is, therefore, to investigate the effect of third order coma on the diffraction images of an incoherent annulus object.

2. Theory

The image spectrum $I(\omega, \Theta)$ is related to the object spectrum $0(\omega)$ by

$$I(\omega, \Theta) = T(\omega, \Theta)\cdot 0(\omega), \tag{1}$$

where ω is the dimensionless spatial frequency variable, Θ is the corresponding azimuthal angle in the Fourier transform space, and $T(\omega, \Theta)$ is the transfer function of the optical system under consideration.

The image intensity distribution $i(V, \chi)$, which is the inverse Fourier transform of $I(\omega, \Theta)$, is given by

$$i(V, \chi) = (1/2\pi) \int_0^2 \int_0^2 T(\omega, \Theta)\cdot 0(\omega) \times \times \exp\big(iV\omega\cos(\Theta-\chi)\big)\omega\, d\omega\, d\Theta, \tag{2}$$

where V and χ are the polar coordinates in image plane, χ defines the measurement direction, and V is a dimensionless distance parameter related to the parameters of the optical system by

$$V = \frac{(\pi D \sin a)}{\lambda}.$$

Here D is diameter of the aperture, λ is wavelength of light, and a is the semifield angle.

The object spectrum for an annular target is given [47] by

$$0(\omega) = \frac{\sigma_2^2 J_1(\sigma_2\omega)}{\sigma_2\omega} - \frac{\sigma_1^2 J_1(\sigma_1\omega)}{\sigma_1\omega}. \tag{3}$$

Here σ_1 and σ_2 are the inner and outer radii of the annulus in reduced units.

The optical transfer function for circular aperture systems in presence of coma has been calculated by many workers [15, 20]. We have followed the approach of Barakat and Houston [20], its brief outline of the same is given below.

The optical transfer fuction of a system can be written as the autocorrelation of its pupil function. Thus

$$T(\omega_p, \omega_q) = [T(0,0)]^{-1} \iint A(p+\tfrac{1}{2}\omega_p, q+\tfrac{1}{2}\omega_q) \times \times A^*(p-\tfrac{1}{2}\omega_p, q-\tfrac{1}{2}\omega_q)\, dp\, dq, \tag{4}$$

where $A(p,q)$ is the pupil function, $A^*(p,q)$ its complex conjugate, ω_p and ω_q the spatial frequency variables, and p, q optical direction cosines in exit pupil plane. In the case of a system suffering from aberration, the pupil function, defined as the amplitude distribution in the pupil plane, may be written as

$$A(p,q) = \begin{cases} 0 & \text{for } p^2+q^2 > 1 \\ \exp\big(ikW(p,q)\big) & \text{for } p^2+q^2 < 1 \end{cases} \tag{5}$$

where $W(p,q)$ is the aberration function. For the case of primary coma, it is given by

$$W(p,q) = W_{31} q(p^2+q^2). \tag{6}$$

Here the aberration coefficient W_{31} gives the number of wavelengths of aberration present. It is convenient, following Hopkins [36], to reduce the problem to a single frequency variable by the transformation

$$p = \alpha\cos\Theta - \beta\sin\Theta,$$
$$q = \alpha\sin\Theta + \beta\cos\Theta. \tag{7}$$

Thus

$$T(\omega, \Theta) = [T(0,0)]^{-1} \iint A(\alpha+\tfrac{1}{2}\omega, \beta) \times \times A^*(\alpha-\tfrac{1}{2}\omega, \beta)\, d\alpha\, d\beta, \tag{8}$$

where the new set of spatial frequency variables ω, Θ is given by

$$\omega = (\omega_p^2+\omega_q^2)^{1/2}, \quad \Theta = \tan^{-1}(\omega_p, \omega_q). \tag{9}$$

Thus, the transfer function becomes

$$T(\omega, \Theta) = T_r(\omega, \Theta) + iT_i(\omega, \Theta), \tag{10}$$

where

$$T_r(\omega, \Theta) = [T(0,0)]^{-1} \int_{-a}^{a}\int_{-b}^{b} \cos[2\pi W(\alpha+\tfrac{1}{2}\omega, \beta) - -2\pi W(\alpha-\tfrac{1}{2}\omega, \beta)]\, d\alpha\, d\beta, \tag{11a}$$

$$T_i(\omega, \Theta) = [T(0,0)]^{-1} \int_{-a}^{a}\int_{-b}^{b} \sin[2\pi W(\alpha+\tfrac{1}{2}\omega, \beta) - -2\pi W(\alpha-\tfrac{1}{2}\omega, \beta)]\, d\alpha\, d\beta, \tag{11b}$$

and the limits of investigation a, b are

$$a = (1-\tfrac{1}{4}\omega^2)^{1/2},$$
$$b = (1-\beta^2) - \tfrac{1}{2}\omega. \tag{12}$$

From (5) and (6) we have

$$W(\alpha+\tfrac{1}{2}\omega, \beta) - W(\alpha\tfrac{1}{2}\omega, \beta) = 4\pi W_{31}[\tfrac{1}{8}\omega^3\sin\Theta + \tfrac{3}{2}\alpha^2\omega\sin\Theta + \tfrac{1}{2}\omega\beta^2\cos\Theta - \alpha\beta\omega\sin\Theta]. \tag{13}$$

With the help of expression (13) expressions (11a) and (11b) can by evaluated.

Therefore, the final expression for evaluating the intensity distribution is

$$i(V, \chi) = \int_0^2 \int_0^2 0(\omega)\big[T_r\cos\big(V\omega\cos(\Theta-\chi)\big) + T_i\sin\big(V\omega\cos(\Theta-\chi)\big)\big]\omega\, d\omega\, d\Theta, \tag{14}$$

where $0(\omega)$, T_r, T_i are given by equations (4), (11a), (11b), respectively.

3. Results and discussion

The integral occurring in equation (14) being not easily amenable to analytic evaluation, a 32-point Gauss quadrature method is used to solve it numerically on an ICL 1909 computer. The intensity distributions were calculated for the values of aberration coefficient W_{31} equal to 0.25, 0.50, 0.75, 1.0, 1.5 and 2.0, and the results obtained in the paraxial receiving plane along three azimuths viz. $\chi = 0$, $\pi/4$ and $\pi/2$. The outer radius of the annulus was taken to be three times greater than the inner radius, i.e. $\sigma_2 = 3\sigma$, $\sigma_1 = \sigma$. All the results of intensity distributions have been plotted graphically in figs. 1–12. The curves is

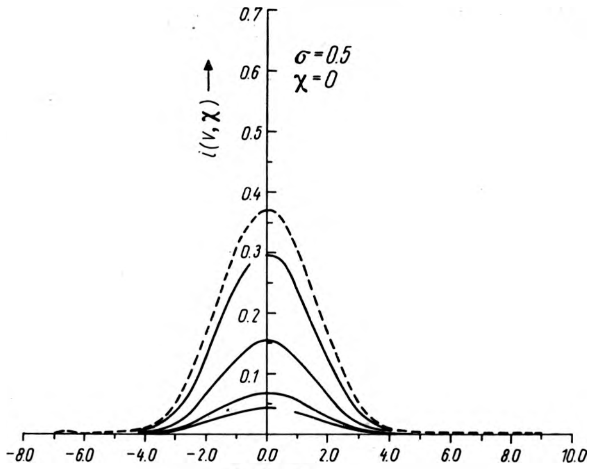

Fig. 1. Diffraction images of an incoherent annulus for different amount of aberration (dotted curve shows the aberration free case) for $\sigma = 0.5$ and $\chi = 0$

$W_{31} = 1 - 0.25$, $2 - 0.50$, $3 - 0.75$, $4 - 1.0$,

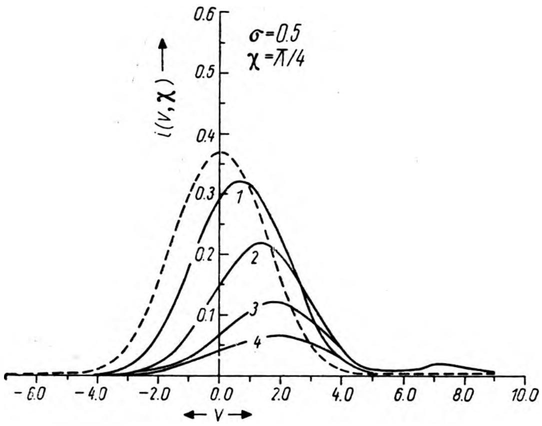

Fig. 2. Diffraction images of an incoherent annulus for different amount of aberration (dotted curve shows the aberration free case) for $\sigma = 0.5$ and $\chi = \pi/4$

$W_{31} = 1 - 0.25$, $2 - 0.50$, $3 - 0.75$, $4 - 1.0$

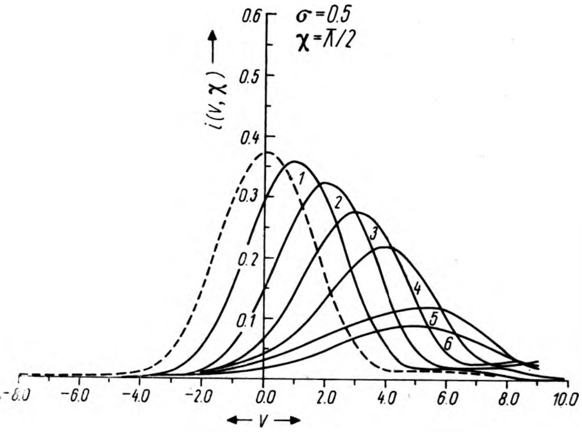

Fig. 3. Diffraction images of an incoherent annulus for different amount of aberration (dotted curve shows the aberration free case) for $\sigma = 0.5$ and $\chi = \pi/2$

$W_{31} = 1 - 0.25$, $2 - 0.50$, $3 - 0.75$, $4 - 1.0$, $5 - 1.5$, $6 - 2.0$

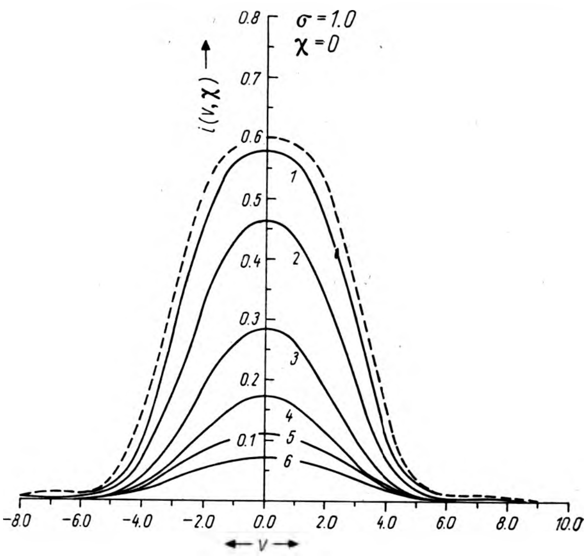

Fig. 4. Diffraction images of an incoherent annulus for different amount of aberration (dotted curve shows the aberration free case) for $\sigma = 1.0$ and $\chi = 0$

$W_{31} = 1 - 0.25$, $2 - 0.50$, $3 - 0.75$, $4 - 1.0$, $5 - 1.5$, $6 - 2.0$

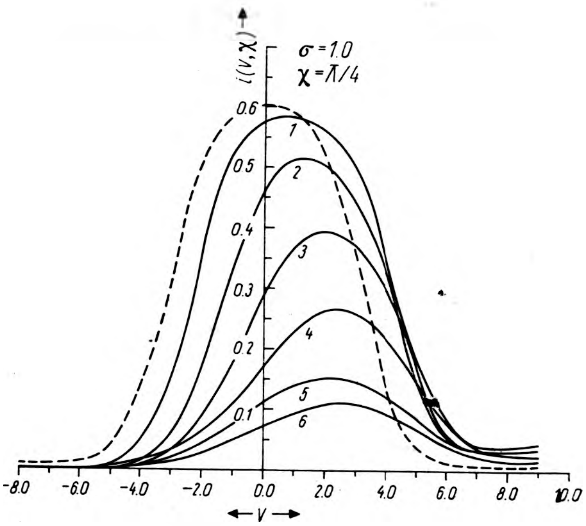

Fig. 5. Diffraction images of an incoherent annulus for different amount of aberration (dotted curve shows the aberration free case) for $\sigma = 1.0$ and $\chi = \pi/4$

$W_{31} = 1 - 0.25$, $2 - 0.50$, $3 - 0.75$, $4 - 1.0$, $5 - 1.5$, $6 - 2.0$

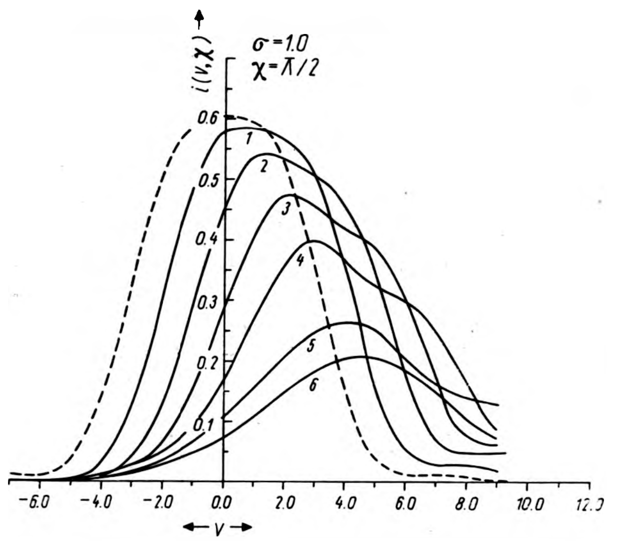

Fig. 6. Diffraction images of an incoherent annulus for differen amount of aberration (dotted curve shows the aberration free case for $\sigma = 1.0$ and $\chi = \pi/2$

W_{31} = *1* – 0.25, 2 – 0.50, *3* – 0.75, *4* – 1.0, *5* – 1.5, *6* – 2.0

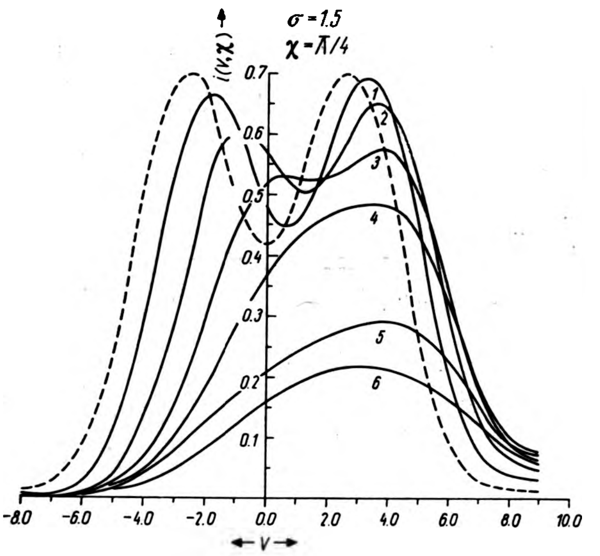

Fig. 8. Diffraction images of an incoherent annulus for different amount of aberration (dotted curve shows the aberration free case) for $\sigma = 1.5$ and $\chi = \pi/4$

W_{31} = *1* – 0.25, *2* – 0.50, *3* – 0.75 *4* – 1.0, *5* – 1.5, *6* – 2.0

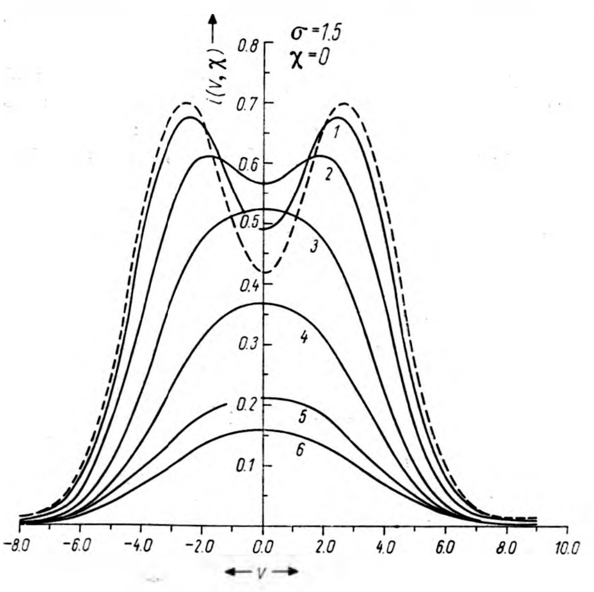

Fig. 7. Diffraction images of an incoherent annulus for different amount of aberration (dotted curve shows the aberration free case) for $\sigma = 1.5$ and $\chi = 0$

W_{31} = *1* – 0.25, *2* – 0.50, *3* – 0.75, *4* – 1.0, *5* – 1.5, *6* – 2.0

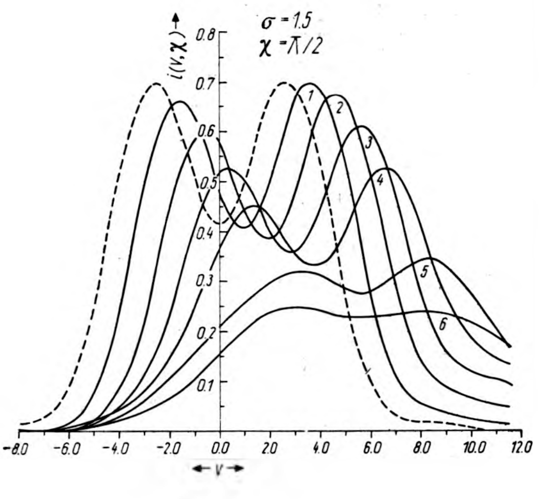

Fig. 9. Diffraction images of an incoherent annulus for different amount of aberration (dotted curve shows the aberration free case) for $\sigma = 1.5$ and $\chi = \pi/2$

W_{31} = *1* – 0.25, *2* – 0.50, *3* – 0.75, *4* – 1.0, *5* – 1.5, *6* – 2.0

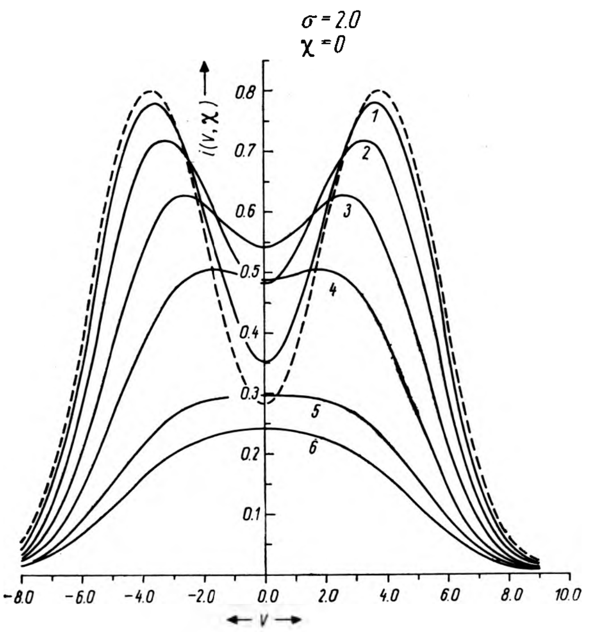

Fig. 10. Diffraction images of an incoherent annulus for different amount of aberration (dotted curve shows the aberration free case) for $\sigma = 2.0$ and $\chi = 0$

W_{31} = *1* — 0.25, *2* — 0.50, *3* — 0.75, *4* — 1.0, *5* — 1.5, *6* — 2.0

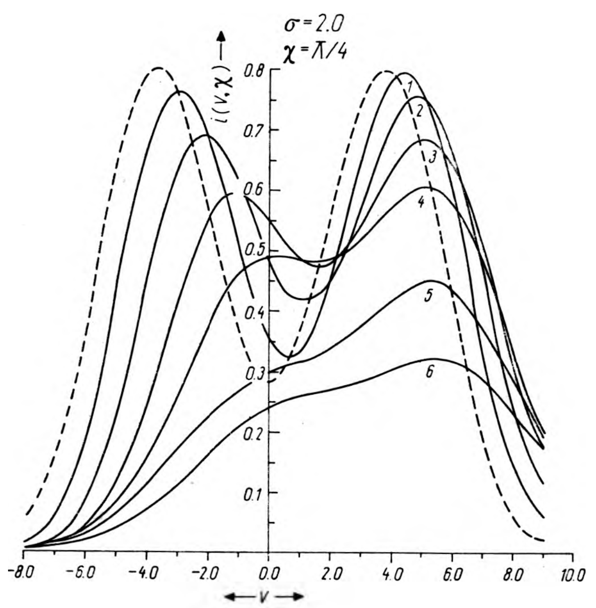

Fig. 11. Diffraction images of an incoherent annulus for different amount of aberration (dotted curve shows the aberration free case) for $\sigma = 2.0$ and $\chi = \pi/4$

W_{31} = *1* — 0.25, *2* — 0.50, *3* — 0.75, *4* — 1.0 *5* — 1.5, *6* — 2.0

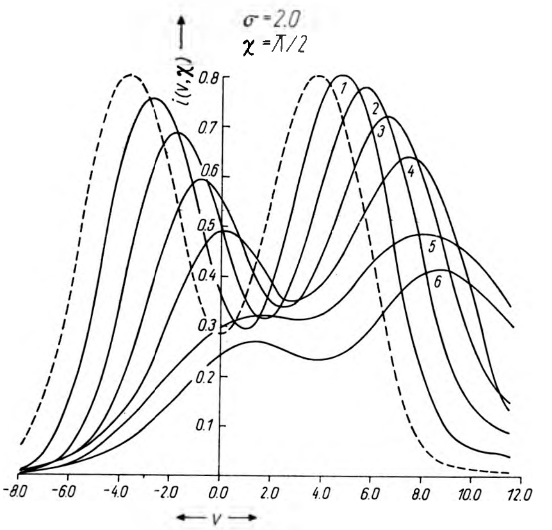

Fig. 12. Diffraction images of an incoherent annulus for different amount of aberration (dotted curve shows the aberration free case) for $\sigma = 2.0$ and $\chi = \pi/2$

W_{31} = *1* — 0.25, *2* — 0.50, *3* — 0.75, *4* — 1.0, *5* — 1.5, *6* — 2.0

aberration free case are shown by dotted lines in all the figures and these are in agreement with the results published by previous authors [54, 59].

Decrease in intensity, resulting diffraction broadening and shift of peak intensity point from the origin have been shown in various cases for different amounts of aberrations (figs. 1–12). However there in no shift along the azimuth $\chi = 0$. It increases as we go along other directions, and becomes maximum for $\chi = \pi/2$. It is worth mentioning that shift in the position of peak intensity causes a measurement error [65] when optical instruments suffering from asymmetric aberrations, such as coma are used. Our graphical results give directly the amount of shift, and hence may be useful. In the words of Hopkins and Dutton [66]

> "It is interesting to note that lens designers have avoided the phase problem of OTF by penalizing unsymmetrical imagery. Their automatic correcting programms have strong tendencies to eliminate these kinds of errors. The lens testing community, however, is faced with lenses which have decentring errors due to manufacture, which introduces unsymmetrical images. The phase term cannot be ignored for it most certainly degrades the lens performance. The irony of situation is if lens designers eliminate unsymmetrical image errors, they often design lenses which are sensitive to tilt and decentre. The manufactured lenses then have unsymmetrical image errors which the testing people also want to ignore. This divergent looping needs closing".

It is also observed that for small values of σ the image of an annulus object is similar to that of a disk object. For large σ it resembles more and more the objects. However, is presence of aberration it may be mistaken as due to a disk object even for longe values of σ. For example for $\sigma = 1.5$ and $W_{31} = 0.5$ the image can be identified as that due to an annulus object, whereas for $W_{31} = 1.0$ this is likely to be interpretated as that of disk object. It is also inferred that the image of an annulus may be derived as the difference of two disk images of various diameters. It holds good in presence of aberration too.

Charman [51] has discussed the contrast transfer function for the annulus target, for which the convention is that spatial frequency is the reciprocal of the mean diameter of the annulus. The results can be generalized for the present case by taking some more values of σ. As reported by earlier workers [59] the image of an incoherent annular object on a light background is complementary to that of a bright annular object on a dark background. This also holds in presence of aberration.

Hence, we conclude that the presence of aberration distorts the object and one is likely to mislocate the object. Thus this fact should be taken into consideration by those engaged in interpretation of photographs in aerial reconnai:sance work. Such studies are also useful in developing an image simulation programme, as done by Paris [63].

It is also interesting to note that equation (14) is analogous to the expression for Fraunhofer diffraction pattern with partially coherent illumination [67]. Therefore our results will be valid for imagery under partial coherent light for the correlation

$$\gamma(a\varrho) = \left[\frac{2J_1(a\varrho)}{a\varrho} - 2\varepsilon^2 \frac{J_1(\varepsilon a\varrho)}{\varepsilon a\varrho}\right], \qquad (15)$$

where the symbols have the same meaning as in paper [67].

4. Future work

The problem of restoring the images degraded by non-symmetric aberrations, such as coma and astigmatism, is currently receiving our attention. Techniques of processing by computer-generated filters using fast Fourier transform seems to be very promising. In a future paper we hope to report our findings in this direction. The effect of balancing of aberrations [29, 33] on the diffraction images under partially coherent illumination is being studied. The joint influence of linear coma and partial coherence due to atmospheric turbulence on the far-field diffraction patterns of circular aperture is also being investigated.

*

* *

The authors wish to thank Professors M. De and M. S. Sodha for encouragement. Useful discussion with and help received from Shri. R. N. Singh are gratefully acknowledged.

Дифракционная теория образования изображения в присутствии линейной комы: кольцевой некогерентный предмет

Исследовался кольцевой некогерентный предмет в присутствии линейной комы (круговой), применяя метод оптической функции переноса. Результаты приведены для параксиальной плоскости изображения при разных значениях комы и разных размерах предметов. Вычерчены были отклонения от вращательной симметрии, происходящие в полученных изображениях, и обсуждены были другие вредные последствия аберрации. В заключительной части работы намечена программа дальнейших исследований.

References

[1] Martin L. C., Month. Not. Roy. Astro. Soc. **82,** 1922, p. 310.
[2] Steward G. C., *The Symmetrical Optical System,* Cambridge University Press, London 1928, p. 81.
[3] Nijboer B. R. A., *Diffraction Theory of Aberrations,* Thesis, Groningen 1942.
[4] Nijboer B. R. A., Physica **13,** 1947, p. 605.
[5] Nienhuis K., *Image Formation in the Pressence of Aberrations,* Thesis, Groningen 1948.
[6] Kingslake R., Proc. Phys. Soc., **61,** 1948, p. 147.
[7] Nienhuis K., Nijboer B. R. A., Physica **14,** 1949, p. 590.
[8] Van Kampen N. G., Physica **14,** 1949, p. 545.
[9] Van Kampen N. G., Physica **16,** 1950, p. 617.
[10] Steel W. H., Rev. d'Opt. **32,** 1953, p. 143.
[11] Linfoot E. H., *Recent Advances in Optics,* Oxford University Press, London 1955.
[12] De M., Nath B. K., Optik **15,** 1958, p. 739.
[13] Miyamato K., J. Opt. Soc. Am. **57,** 1958, p. 567.
[14] Marathy A. S., Proc. Roy. Soc. **74,** 1959, p. 727.
[15] Goodbody A. M., Proc. Phy. Soc. **76,** 1960, p. 677.
[16] Charoenkul P., Proc. Phy. Soc. **86,** 1965, p. 213.
[17] Kapany N. S., Burke J. J., J. Opt. Soc. Am. **52,** 1962, p. 1351.
[18] Barakat R., Houston A., J. Opt. Soc. Am. **54,** 1964, p. 1084.
[19] Barakat R., Houston A., J. Opt. Soc. Am. **55,** 1965, p. 1132.
[20] Barakat R., Houston A., J. Opt. Soc. Am. **55,** 1965, p. 1142.
[21] Develis J. B., J. Opt. Soc. Am. **55,** 1965, p. 1632.
[22] Barakat R., Houston A., J. Opt. Soc. Am. **56,** 1966, p. 1402L.
[23] Asakura T., Mishina H., Jap. J. Appl. Phys. **7,** 1968, p. 751.
[24] Yzuel M. J., Hopkins H. H., Opt. Acta **17,** 1970, p. 157.
[25] MacDonald J., Opt. Acta **18,** 1971, p. 269.
[26] Powell I., Opt. Acta **20,** 1973, p. 879.
[27] Welford W. T., *Aberrations of the Symmetrical Optical System,* Academic Press, London 1974.
[28] Bezdid'ko S. N., Sov. J. Opt. Tech. **41,** 1974, p. 475.
[29] Gostick R. W., Thesis University of London, 1974.
[30] Ishii Y., Kubota T., Opt. Commun. **10,** 1974, p. 250
[31] Yoshida A., Asakura T., Opt. Commun. **14,** 1975, p. 211
[32] Biswas S. G., Boivin A., J. Opt. Soc. Am. **65,** 1975, p. 1225A.
[33] Gostick R. W., Opt. Quant. Electron. **8,** 1976, p. 31.
[34] Yzuel M. J., Bescos J., Opt. Acta **23,** 1976, p. 329.

[35] De M., Proc. Roy. Soc. A **223,** 1955, p. 91.
[36] Hopkins H. H., Proc. Phys. Soc. **70B,** 1957, p. 449.
[37] Montgomery A. J., J. Opt. Soc. Am. **56,** 1966, p. 622.
[38] Singh K., Rattan R., J. Optics (India) **3,** 1974, p. 60.
[39] Chandra A., Singh K., Singh R. N., Atti. Fond G. Ronchi, **30,** 1975, p. 703.
[40] Chandra A., Singh K., Atti. Fond. G. Ronchi **30,** 1975, p. 341.
[41] Biswas S. C., Boivin A., J. Optics (India) **4,** 1975, p. 1.
[42] Brock G. C., *The Physical Aspects of Aerial Photography,* Dover Publication, Inc. New York. 1967.
[43] Dainty J. C., Shaw R., *Image Science,* Academic Press, London 1974.
[44] Shaw R., Ed. *Selected Reodings in Image Evaluation,* SPSE Washington 1976.
[45] Shaw R., Ed. International Conference on Image Analysis and Evaluation, SPSE Washington 1976.
[46] Barakat R., Houston A., J. Opt. Soc. Am. **54,** 1964, p. 768.
[47] Barakat R., Houston A., J. Opt. Soc. Am. **55,** 1965, p. 881.
[48] Barakat R., Opt. Acta **16,** 1969, p. 405.
[49] Gupta P. C., Singh K., Appl. Opt. **15,** 1976, p. 2233.
[50] Rattan R., Singh K., Nouv. Rev. D'Optique **7,** 1976, p. 259.
[51] Charman W. N., Photo. Sci. Engn. **8,** 1964, p. 253.
[52] Charman W. N., Canadian Surveyor **19,** 1965, p. 190.
[53] Howlett L. E., Cand. J. Res. **A24,** 1946, p. 15.
[54] Hariharan P., J. Opt. Soc. Am. **45,** 1955, p. 44.
[55] Hariharan P., J. Opt. Soc. Am. **45,** 1955, p. 60.
[56] Hariharan P., J. Opt. Soc. Am. **46,** 1956, p. 315.
[57] Hariharan P., Photo. Sci. Engn. **2,** 1958, p. 177.
[58] Carman P. D., Charman W. N., J. Opt. Soc. Am. **54,** 1964, p. 1121.
[59] Som S. C., J. Opt. Soc. Am. **57,** 1976, p. 1499.
[60] Rattan R., Singh K., Nouv. Rev. D'Opt. **6,** 1975., p. 223.
[61] Singh K., Jagpal Singh, Maggo J. N., Ind. J. Pure and Appl. Phys. **13,** 1975, p. 840.
[62] Rattan R., Singh K., Pramana **6,** 1976, p. 109.
[63] Image Simulation Program (IMSIM), Optical Research Associate, U.S.A. (Developed by D.P. Paris of IBM).
[64] Artishevskii V. I., Gradoboev V. M., Sov. J. Opt. Tech. **42,** 1975, p. 672.
[65] Sokol'skiy M. N., Sov. J. Opt. Tech. **39,** 1972, p. 538.
[66] Hopkins R. E., Dutton D., Photogram. Engn. **39,** 1973, p. 275.
[67] Singh K., Dhillon H. S., J. Soc. Opt. Soc. **59,** 1969, p. 395.

Received November 15, 1976